Concrete Samples Extracted from Pile Caps and Affected by Internal Swelling Reactions: A Diagnostic Analysis

N. Nascimento, F. A. N. Silva, A. C. Azevedo, T. Mahfoud, A. Khelidj, and João M. P. Q. Delgado

Abstract In this work, it was analyzed in detail the problem of the extensive cracking in the pile cap foundation originated by the delayed ettringite formation, possibly from a high heat of hydration coming from the concreting of the large volume of concrete. Laboratory tests were performed to evaluate the transport properties of concrete samples, as well as their physical and chemical composition using advanced analyses. The tests performed were apparent porosity, gas permeability, scanning electron microscopy, X-ray diffraction and Raman spectroscopy. The presence of crystalline products of the alkali-aggregate reaction was proven through physical–chemical analyses, such as Raman spectroscopy and EDS. As well as the ettringite crystals found in XRD standards, SEM images and the chemical composition of EDS. The porosity showed a high value (between 9 and 10%), as well as the concrete permeability (10^{-16} and 10^{-15}), determining the negative influence of ISR on the transport properties. Therefore, the methods used have proven to be effective in understanding the problem encountered and have the potential to be used in the design and execution of pile cap blocks.

N. Nascimento · F. A. N. Silva
Department of Civil Engineering, Universidade Católica de Pernambuco, Recife, Brazil
e-mail: fernando.nogueira@unicap.br

T. Mahfoud · A. Khelidj
GeM Laboratory, University of Nantes, Saint Nazaire, Nantes, France
e-mail: mahfoud.tahlaiti@icam.fr

A. Khelidj
e-mail: abdelhafid.khelidj@univ-nantes.fr

A. C. Azevedo · J. M. P. Q. Delgado (✉)
CONSTRUCT-LFC, Departamento de Engenharia Civil, Universidade do Porto, Rua Dr. Roberto Frias, s/n, 4200-465 Porto, Portugal
e-mail: jdelgado@fe.up.pt

A. C. Azevedo
e-mail: antonio.costaazevedo@fe.up.pt

1 Introduction

In the last decade, the occurrence of early deterioration of pile cap blocks in residential buildings and concrete bridges in the Metropolitan Region of Recife has been reported with relative frequency. This process usually starts with the occurrence of a horizontal crack of large opening in the lateral faces of the element, located approximately 30 cm from the upper face of the block, and its installation is usually attributed to the expansions of concrete resulting from the alkali-silica reaction.

The pathological manifestations associated with chemical phenomena are more common all over the world in construction works containing large volumes of concrete, such as dams and pavements [1], but in Brazil, especially in the northeast of the country, the occurrence of alkali-silica reaction (ASR) and delayed ettringite formation (DEF) in pile cap blocks and in spread footing foundations of residential buildings and bridges at early ages is very common. This fact has payed the attention of the civil construction industry and local research centers to the need to understand the mechanisms involved in this process so that mitigating or corrective measures can be adopted.

Several authors presented studies of the occurrence of alkali-silica reaction and the delayed ettringite formation occurring simultaneously. Machoviè et al. [2] analyzed the concrete microstructure through scanning electron microscopy (SEM) and found the two phenomena. Another interesting case was the one presented by Shayan and Morris [3] in which visual inspection and analysis identified the ASR, mainly because in the composition of the concrete of the bridge it was found gneiss with reactive quartz. On the other hand, the heat of hydration released during concrete casting around 80 °C caused the DEF.

In an advanced investigation of concrete cores carried out by Hasparyk [4], the two reactions were found, where in addition to visual inspection, several tests were performed, as well as analyses of the microstructure by means of SEM, EDX and XRD. A bridge deck damaged by ASR and DEF studied by Shayan et al. [5] showed significant reductions in the modulus of elasticity, as well as residual expansion. Another foundation structure that presented combined attack was studied by Hasparyk et al. [6], where the causes of the occurrence of these phenomena were the temperature around 80 °C and the presence of reactive aggregates in concrete. A comprehensive understanding of the damage generated by the combination of DEF + ASR presented by Sanchez et al. [7] showed reductions in the mechanical properties of the concrete analyzed.

Many structures in Britain and France that had in their composition high cement consumption (between 420 and 550 kg/m^3) and high equivalent alkali content (> 4.0 kg/m^3) presented several damages between 5 and 20 years after their construction,

in the presence of moisture and in a temperature close to 80 °C, besides being concreted during the summer, which potentiated the heat release [8].

DEF manifests itself when the source of sulfate ions is internal and not external, in the presence of an aggregate contaminated by gypsum or cement with high sulfate content. In addition to these factors, the process of steam-curing the concrete at temperatures above 65 °C can cause the development of delayed ettringite, since it is not stable in these conditions [9].

In concrete submitted to a high temperature during concrete casting in place, it is possible that the primary ettringite formed during the hydration reactions is decomposed [10]. When it returns to room temperature and in the presence of humidity, this ettringite can re-crystallize inside the hardened concrete, causing expansion pressures that are capable of generating cracking, which potentiates damages to the structure.

According to Bensted [9], the causes, the physical–chemical mechanisms and the kinetics of the reaction that originates the DEF are still not fully understood. However, the combination of several factors is of utmost importance for this internal expansion reaction to begin.

Water is an essential factor to produce the reaction, whether in structures that are in contact with water, susceptible to water ingress or exposed to a high humidity level, such as foundations. Other elements described in Guide Technique [11] are the maximum temperature reached by the structure and the time duration in which this temperature is maintained. Thus, if the temperature exceeds 65 °C and other key parameters are present, the probability of occurrence of DEF is high.

Ettringite is a hydrated calcium trisulfoaluminate, so the sulfate and aluminate contents are directly linked to its formation process. A necessary condition is that the cement used contains a sufficient amount of tricyclic aluminates ($3CaO$, Al_2O_3 or C_3A) and sulfates (SO_3). As ettringite is highly soluble in large quantities of alkalis, the use of a type of cement with a lower alkaline content would contribute to the non-occurrence of the reaction [11].

Another recommendation for the delayed ettringite formation not to occur as described in [11] is the use of mineral additions. It was observed that they contribute to a less exothermic concrete, as they reduce the amount of clinker aluminates and end up modifying the type and texture of the moisturizer. The additions indicated are those that have components with latent or pozzolanic hydraulic properties, such as blast furnace slag or fly ash, natural or artificial pozzolana). Finally, the petrographic nature and the volumetric mass of the aggregate are elements which influence heat transfers in the reactions of concrete.

Studies have shown that an isolated factor is not sufficient for the internal expansion reactions to develop, but the presence of several parameters acting simultaneously under certain conditions. Both expansion reactions (ASR and DEF) have similar symptoms and the two have moisture as a conditioning factor to develop expansion. According to Torres and Andrade researchers [8] what may be happening in the Metropolitan Region of Recife is the combination of ASR/DEF attack mechanisms.

One of the important challenges that researchers have to answer is to understand as fully as possible these phenomena of expansion that affect various concrete pile

cap foundations in the region at an early stage and how it is possible to correlate the level of damage generated with the change in strength and deformation properties of concrete and its durability. Furthermore, it is equally important to relate the results of laboratory tests to the situations found in the field so that possible design and construction strategies can be proposed to minimize the possibility of these expansion phenomena take place on concrete. That is why there is a need for a greater understanding of their features and mechanisms.

This work aims to provide a mechanical and transfer properties characterization and the physical–chemical analysis, using advanced techniques to analyze cores extracted from real buildings that have concrete elements affected by internal swelling reactions.

2 Materials and Methods

2.1 Materials

Figure 1 represents the pile cap S(P1 + P8 + P32), with the extraction sites of each core, identified by the notations (SP-01, SP-02, SP-03, SP-04, SP-05 and SP-06). The points identified by (A, B, C and D) are where were extracted the samples of smaller sizes also used for analysis and characterization. All samples were extracted in the direction parallel to the launching of the concrete and only the SP-06 was in

Fig. 1 Place of extraction of the samples in the Pile Cap Block S(P1 + P8 + P32)
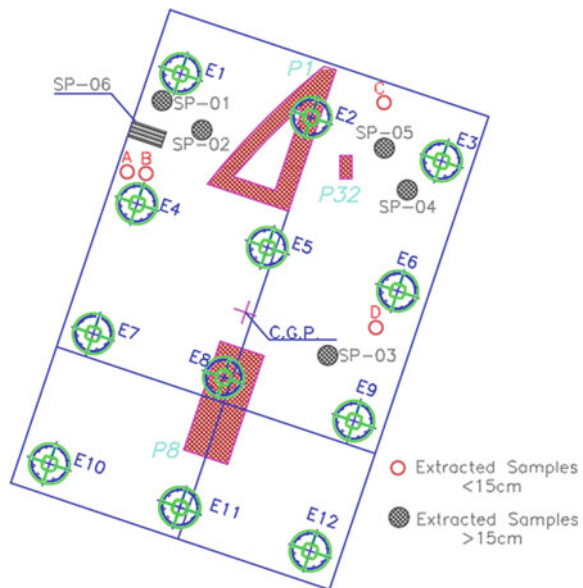
the direction perpendicular to the launching. The face chosen was where there was longitudinal cracking along the pile cap block.

The concrete samples were extracted with two single-phase electric drills of such dimensions with 75 mm diameter—Model Husqvarna dm2 240 and Tyrolit dk32. The extraction procedure was executed in such a way that the sectioning of the block reinforcements was avoided as much as possible. The specimens were extracted from the upper part and from lateral faces of the pile cap block, totalling 6 (six) cylindrical concrete samples with dimension of $15.0 \times 7.5 \, cm^2$—height and diameter, respectively. The entire sample extraction process was performed in a single day and lasted approximately 7 h (see Fig. 2).

The laboratory tests were carried out partly in the facilities of the Institut Catholique D'Arts et Métiers and other partly in the GeM—Institut de Recherche en Génie Civil et Mécanique—UMR 8183—CNRS—École Centrale de Nantes—Université de Nantes.

After choosing the parameters for characterization and diagnosis of pathological manifestations in concrete, the samples were separated, identified and prepared. In the field, it is necessary that the cores are removed from the structure to be studied. Some tests required specific treatments on the samples collected. In some cases, the sample needs to be reduced to very small sizes or even pulverized.

Fig. 2 Samples extracted from the block (SP-01 to SP-06)

A visual analysis was performed to identify possible characteristics of the internal expansion reactions and they were directed to the tests to be performed. Then, a characterization of the concrete samples affected by the reaction was performed with destructive tests and analyses.

2.2 Laboratory Tests

2.2.1 Gas Permeability and Apparent Porosity

The permeability test was performed on two concrete specimens of the pile cap block. A sample (P-02) was taken from the fragments extracted from the SP-01 sample and the sample (P-01) was separated from the point A. They were rectified and left in the dimensions 5×7 cm^2. The specified cell size of the permeability equipment ("debitmètre massique") was 10 cm in diameter, so the samples were wrapped in black silicone resin and placed in a rigid cylindrical mold.

This resin also had the function of waterproofing the lateral surface of the samples. Figure 3a illustrates how the concrete samples were ready for the test. The concrete gas permeability measurement test is easy and quick to perform and its results are important for assessing the durability of the material. These aspects should be considered so that its use can be more widespread in the practice of concrete structure execution.

To obtain the dry mass of the samples, it was chosen to dry them at a temperature of 60 °C in the oven until the mass was stabilized. The dry mass of the samples is obtained when the loss of relative mass of 24 h does not exceed 0.05%. Every day for twelve days the weight of the samples was measured until the stabilization.

The complete apparatus of the permeability equipment ("debitmètre massique") used in the test is shown in Fig. 3b. The intrinsic permeability is measured through a permeameter, with nitrogen being the neutral percolating gas. A manometer reads

Fig. 3 a Samples P-01 and P-02 prepared for the air permeability test; **b** flowmeter massique equipment; **c** system used for the apparent porosity test

the relative pressure (Pi-Patm) applied to the sample. Laboratory temperature and humidity are controlled (T = 17.8 °C and RH = 76%).

After the concrete air permeability tests have been performed, all the water-proofing resin and the apparatus used were removed to put the samples back in the oven until the mass stabilization. To obtain the dry mass of the samples, it was chosen to dry them at a temperature of 60 °C in the oven until the mass was stabilized. The dry mass of the samples is obtained when the loss of relative mass of 24 h does not exceed 0.05%. Every day for one month the weight of the samples was measured until the stabilization.

After the stabilization of the mass has occurred by drying in the oven, the samples were wrapped in a white absorbent tissue covered with a transparent plastic, from which it was possible to remove the air present in the sample and the environment with a vacuum pump. The vacuum pump was then stopped for five minutes to check if air was coming out, as the device was well sealed, suction continued for another 48 h. After this period of time the air suction process was interrupted to introduce water into the apparatus and consequently into the samples.

Figure 3c shows the devices used for porosity tests, where you can see that at one end you have the place where the vacuum pump for air suction is installed and at the other end the water inlet is located. 48 h later, the water end was opened and it was placed the hose in a tank with water, reconnected the vacuum pump that began sucking the water until the whole system was filled. After 72 h the sample was taken and its weight was measured.

2.2.2 Scanning Electron Microscopy (SEM)

The SEM used for observations is a ZEISS ЄVO®40 equipped with a Back-scattered Electron (BSE) detector to determine the chemical composition. The microscopic examinations were carried out on fresh fractures sections on concrete specimens. The specimens were coated with a gold deposit for observations using the SEM in High-Vacuum (HV) mode.

The samples were analyzed by scanning electron microscopy and the spectrum obtained with EDX showed the chemical composition existing in each part analyzed. Some images showed only the morphology of the ettringite or other observed component.

2.2.3 X-Ray Diffraction (XRD)

Through the X-ray diffraction it is possible to obtain the detailed information of the atomic and molecular structure of materials. When a material is exposed to X-rays, a specific peak pattern of the mineral is generated. The ordinate provides the diffraction angle, which corresponds to the spacing of the crystalline arrangement. In the abscissa we see the intensity of the diffracted ray, which is proportional to its quantity in a composite sample and each peak is equivalent to a type of mineral.

XRD patterns were obtained by using an X-ray diffractometer SEIFERT MZ VI E with Co Ka radiation. Measures were done on the bulk powdered samples.

2.2.4 Raman Spectroscopy

The Raman displacement band, that is, the difference in energy between the incident and the scattered, is typically described as a wave number (wavenumber). The most used unit is 1/cm, this is equivalent to joule divided by conversion factor (hc), where h is Planck constant and c is the speed of light.

The sample selection criteria for analysis by Raman spectroscopy were: fragments of the extracted concrete samples with apparent gel edges, pores filled with ettringite and white spots inside the aggregates.

An acrylic resin PRESI Powder KM-U with a liquid catalyst PRESI KM-U suitable for this type of cold resin was used in the concrete samples. The function of resin was to allow the sample to remain flat, allowing the analysis in Raman. After placing the resin in the mold with the sample, it waited 10 min until it warmed up and hardened, and then the sample was polished on #320 silicon carbide paper and then on #120 paper in a specific machine until the surface was polished and flat. The Raman spectra were produced using the Confocal Raman Microscope SENTERRA II (Bruker) with Opus Software, 532 m wavelength laser, 20 mW power, 50× magnification, 20 s integration time with two accumulations.

3 Results and Discussion

Before starting the discussion about the results of the lab tests performed it is important to highlight that the pathological manifestations observed in the foundation block studied probably come from a variety of sources: structure design decisions, definition of materials to be used in the production of the concrete used and care in large volume concrete operations.

3.1 Visual Inspection

Visual inspections were performed on the pile cap block itself as well as on the concrete samples extracted to identify naked eye signs of expansive reactions or chemical attacks to the concrete. From these inspections, it was possible to observe to see features of these expansion reactions already in place by observing the cracking in map forms on the external surface of the pile cap block. It is worth mentioning that at the time of the extraction a report had already been made to detect the causes of degradation, as well as several tests and analyses, and the pile cap block was in the process of recovery (see Fig. 4).

The samples were first visually examined in order to find clues of chemical attacks to concrete such as AAR and DEF. Macroscopically, gel edges from the alkali-silica reaction were observed in the aggregates. Cracks on the coarse aggregates, following to the cement paste, were observed as well as cracks on transition zone reaching the larger pores.

At some locations it was possible to observe detachment between the aggregate and the paste. Some aggregates contained a kind of whitish reaction product inside, very close to its extremities and and many dark edges or spots were found around the coarse aggregate.

Several micropores were fulled with ettringite and many pores were completely filled with white material. In some fragments a large amount of white material was found covering the concrete, like as leaching. It was also observed in some larger pores little deposition of white material, a fact also observed by Hasparyk [4] in the visual inspection of concrete cores with alkali aggregate reaction.

In the preparation of some samples for some tests performed it was done polishing and after this process it was possible to find even smaller pores filled with whitish material as well as particles of aggregates with this same characteristic. The results from the visual inspection performed on the extracted specimens are summarized below:

- Alkali-silica gel edges in the aggregates;
- Pores with white material deposited at the bottom;
- White mass in several places in the concrete;
- Pores completely filled with ettringite;
- Cracking in coarse aggregates;
- Dark spots around the aggregate;
- White spots inside the aggregate;
- Leaching;
- White spot covering the concrete, mainly the mortar;
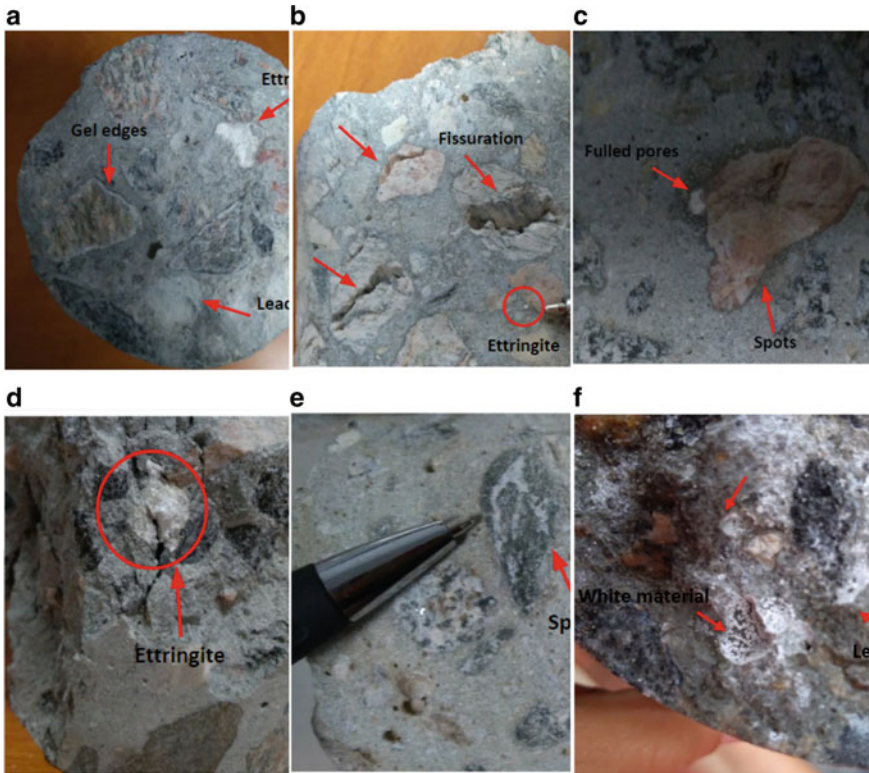- Displacement between the aggregate and the paste;

Fig. 5 Symptoms of the expansion mechanisms found: **a** gel edges; **b** ettringite in the micropores and cracking; **c** spots in the aggregate; **d** pores fulled with ettringite; **e** spots in the aggregate; **f** white material in the pores and leaching

- Cracking in the coarse aggregate following to the transition zone, with the presence of gel in these locations;

Figure 5 shows the main results of the visual inspection performed. The results of visual inspections performed on the concrete samples collected from the block are consistent with a scenario of occurence internal expansion reactions inside the element more compatible with DEF than with the ASR.

3.2 Physical–Chemical Analysis

3.2.1 Gas Permeability and Apparent Porosity

The transfer properties of both healthy and cracked concrete are very important for the study of its durability and porosity and permeability are indicators of this durability.

Table 1 Values of gas permeability and apparent porosity of concrete

Sample	K (m²)	ε (%)
P-01	1.3×10^{-15}	11.29
P-02	3.9×10^{-16}	9.76

Table 1 summarizes the air permeability (K) values for the two samples tested. The results found mean that the concrete samples have a high permeability. In fact, the usual values of this parameter for a concrete are in the range of 10^{-18}–10^{-17} m [12, 13].

This high value of the permeability coefficient can explain the intense cracking process existing in the pile cap block investigated, which allowed the entry of moisture and development of the expansion mechanisms that deteriorated the concrete. The permeability of the samples tested was proportional to the porosity, being higher for P-01. In this sample there was a greater predominance of microcracks. In P-02 there was a large pore, which makes these transport properties smaller.

According to Collepardi [14] the microcracks resulting from the silica alkali reaction in-crease the permeability of concrete, a mechanism that may have contributed to the growth of the values of this property.

Also, from Table 1, the results obtained indicate a high porosity of concrete, a situation also confirmed by its high permeability. This explains the large amount of microcracking found in the field and consequently in the extracted samples. The pore structure of this concrete is then markedly compromised, an aspect that directly interferes with its durability and service life.

One aspect that deserves to be highlighted is that ettringite usually can cause greater expansions in small pores with low connectivity than in larger pores with wide connections [15]. This fact was observed in sample P-02 that presented a large amount of pore in its structure with porosity relatively lower than the P-01 sample that presented a larger amount of microcracks.

It can also be confirmed that ettringite deposited in free pores does not contribute to expansion [16], because in sample P-02 it was found more pores filled with ettringite.

3.2.2 Scanning Electron Microscopy (SEM)

The analysis performed through the scanning electron microstructure allowed the morphology of the samples to be evidenced by means of images. Energy Dispersive X-Ray Spectroscopy (EDX) enables microanalysis, providing chemical composition of the material, which can be used together scanning electron microscopy to get qualified information.

In the analyses performed with SEM, some specific parts that indicated the presence of delayed ettringite formation were chosen. The first point was 309, where the morphology indicated that it was an ettringite acycle. Figure 6a shows this part of the sample, with a magnitude of 1795×.
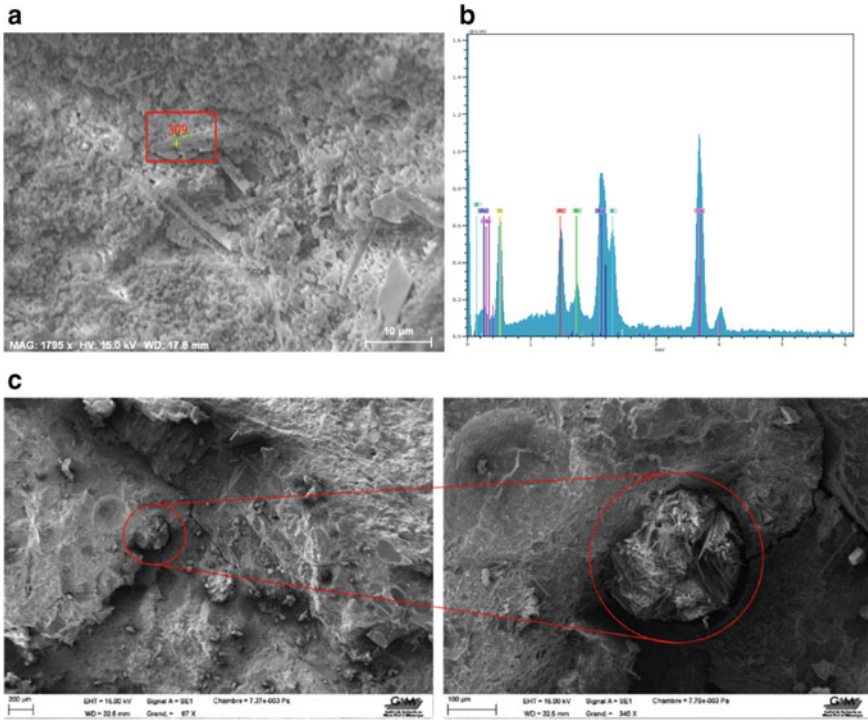
Fig. 6 **a** Acycular crystals of ettringite found in the mortar; **b** components such as: sulphur (S), aluminum (Al) and calcium (Ca) in the sample and **c** ettringite crystals completely filling a pore ($23\times$–$340\times$)

The chemical composition obtained by EDX is shown Fig. 6b, where the components such as Sulfur (S), Aluminum (Al) and Calcium (Ca) suggests the presence of delayed ettringite [4, 17]. Figure 6c illustrates ettringite crystals completely filling an existing pore in the concrete. The first magnitude is $23\times$, being increased to $340\times$.

At point 308 (Fig. 7a) analyzed by SEM, it is possible to observe ettringite crystals developed and deposited in a pore and the corresponding chemical composition is presented in Fig. 7b, with the presence of Sulfur (S), Aluminum (Al) and Calcium (Ca), aspect that confirms that it is delayed ettringite [4].

This particle (point 304—Fig. 8a) analyzed showed in its chemical composition Aluminum (Al), silicon (Si) and sodium (Na), indicating that there are components of delayed ettringite formation and crystalline products of alkaline reaction [4] acting together. Figure 8b illustrates the composition (Al, Si and Na) of this point analyzed.
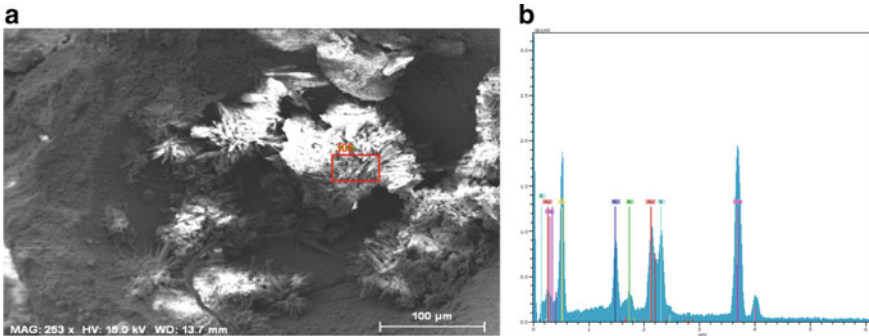
Fig. 7 **a** Ettringite crystals deposited in a pore; **b** chemical composition of the crystals
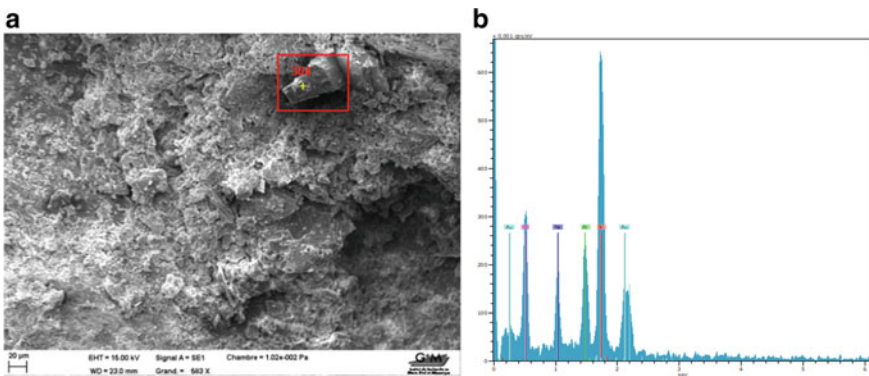

Fig. 8 **a** Aggregate particle with crystalline products of the alkali-silica reaction; **b** crystalline product of alkaline silica reaction

3.2.3 X-Ray Diffraction (XRD)

Through the X-ray diffraction it is possible to obtain the detailed information of the atomic and molecular structure of materials (mainly the crystalline ones).

In the analyses with EDX it was possible to observe a large amount of sulfur (S), aluminum (Al) and calcium (Ca), chemical elements predominantly found in crystals of ettringite [4]. The XRD analyses also proved the presence of ettringite and pyrite (sulphate) internally. These internal compounds associated with a high heat of hydration may have caused the formation of delayed ettringite. Figure 9 shows the patterns of concrete damaged by internal expansion reactions.

The highest peaks are from pyrite, followed by quartz and ettringite. They are similar to those found by [4, 9] in cases of dams affected by delayed ettringite and alkali-silica reaction, respectively. The diffraction angles that showed strong reflection were: 2 theta of 37°, 2 theta of 41° and 2 theta of 55°, with high intensities, and refer to Pirita or Sulfate. The ettringite with greater intensity is found in 2 theta
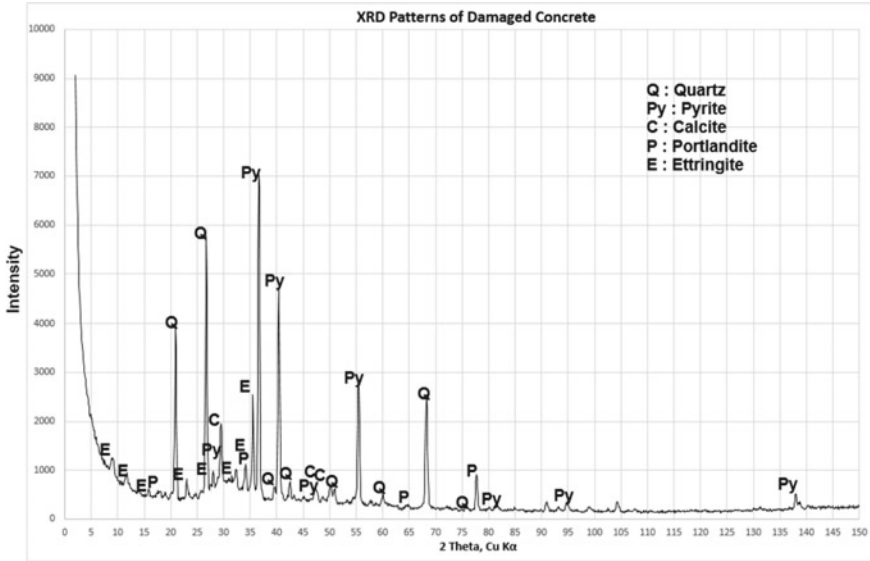
Fig. 9 Presence of pyrite (sulphate), sodium hydroxide, calcium carbonate and silicon dioxide

of 36°, corresponding to the crystals present in all the concrete, predominantly of the pores and voids.

Another high intensity peak also recognized in the diffractometer was the mineral component quartz, corresponding to the crystalline products of the alkali-silica reaction. This mineral appeared more strongly in 2 theta of 21°, 2 theta of 27° and 2 theta of 68°, indicating crystalline phases of the material. These peaks are attributed to the contamination of the paste by the reactive aggregate.

3.2.4 Raman Spectroscopy

Figure 10a represents the coarse aggregate region of the RA-02 sample in expanded resolution. Four points (a, b, c and d) were chosen to be analyzed by Raman spectroscopy.

Figure 10b illustrates the Raman spectra of the crystalline products found in different locations of the same analyzed aggregate. The Raman spectra were found between two wide bands, in the range of 100–600 cm^{-1} (low frequency region), indicating the amorphous nature of the gel. The wave numbers identified (see Fig. 10b) were similar to those found by the researchers for the aggregates that contained reactive mineral [17, 18]. When analyzing the edges of the aggregate, the bands of the crystalline product do not result in peaks, indicating only noises, a similar behavior found in [19]. The colour of the dots corresponds to the colour of the spectra, the corresponding sequence is: b, a, d and c.
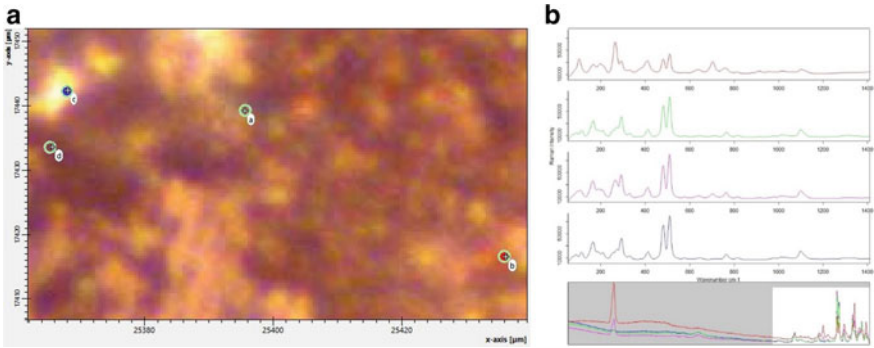
Fig. 10 a Points (a, b, c, d) where the Raman analysis was performed; **b** Raman spectra of the crystalline products at the four points analyzed in the RA-02 sample

In the other samples analyzed, the spectra were not generated, even performing new polishing with silicon carbide (P120), because it showed an increase in noise, causing the signal of the products no longer recognized. In a new analysis in the same sample, now in the blue and red points (see Fig. 11a), different Raman intensities were found, but still in the same wavenumber range. The colour of the dots corresponds to the colour of the spectra.

In Fig. 11b the crystalline product was found in the same range of wave numbers (from 100 to 600 cm^{-1}), being different in peak intensity.

Figure 12a shows the point from which this spectra was obtained and the Fig. 12b shows the spectrum of the crystalline product located inside a pore in the RA-05 sample. There are different peaks, the largest is in the range of 800–1000 cm^{-1}. In
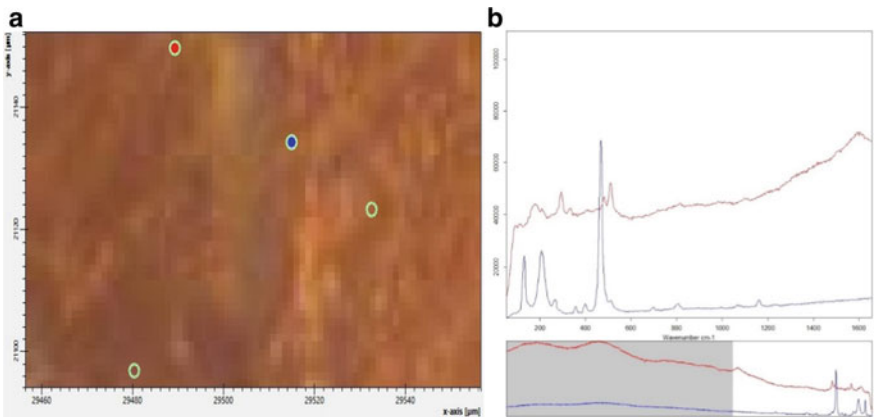

Fig. 11 a Points where the Raman analysis was performed (sample RA-02); **b** range of 100–600 cm^{-1} analyzed
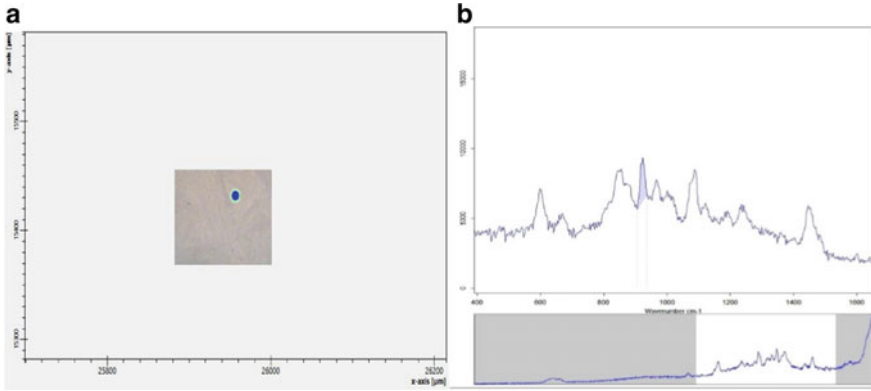
Fig. 12 **a** Crystalline product analyzed by Raman spectroscopy; **b** Raman spectra values found in the ASR products inside a pore

the wavenumber 600 cm^{-1} there is a peak, similar to what was found by [17] as a peak of the alkali-silica reaction product.

The chemical analysis performed with the Raman spectroscopy indicated possible spectra corresponding to the crystalline products of the alkali-silica reaction, which confirmed the presence of sodium in the previously obtained EDX spectra. The reactions (alkali-aggregate reaction and delayed ettringite formation) are acting concomitantly.

In resume, the main findings from the laboratory testing campaign of the extracted samples are presented below.

- High values of porosity were found, between 9 and 11%, explained by the large amount of micro-cracks in the field and in the extracted samples;
- The pore structure was much compromised in this concrete, an aspect that directly interferes with its durability and service life.

In the analysis with SEM, the morphologies identified were those of ettringite acicular crystals in the mortar and also completely filling the pores, illustrated in Fig. 13. In the dispersive energy spectroscopy the following components were obtained: sulfur, aluminum and calcium, characteristic minerals of the ettringite crystals. In the XRD standards these elements were also found, as well as the mineral pyrite (or sulfate) and the ettringite itself. Pyrite was the mineral with the highest peak intensity in the graph, confirming the high presence of DEF in the concrete.

In the microstructure of the concrete there are pores and voids, and as [16] the ettringite crystals accumulate in the available free spaces, and often the ettringite that is deposited there does not contribute to the expansion. Thus, these products resulting from the reaction were deposited in the pores of the concrete and making a tamponade of existing voids. Through the process of pore-filling the pores [4], proven in visual inspections and SEM analyses, the compressive strength of the concrete showed high values. The cracking on a map of the block in its surface did
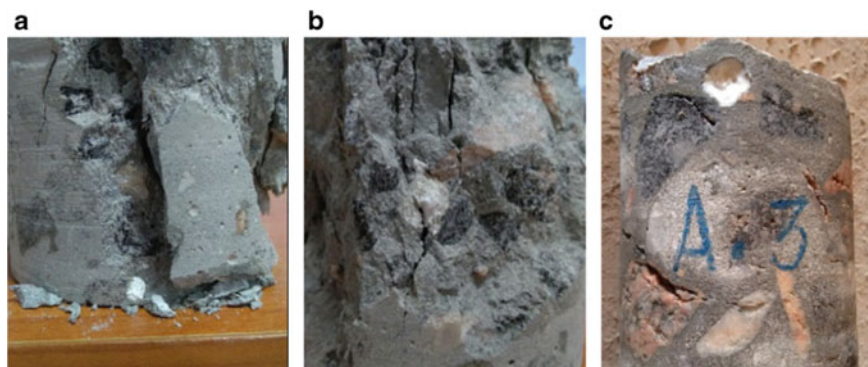
Fig. 13 Pores completely filled with ettringite crystals: **a** and **b** concrete sample after compressive rupture; **c** concrete sample after extraction

not happen in the whole block, but in half of it. The AM-02 sample presented a lower strength value compared to the other two because it was extracted from a location of the block where there was little apparent cracking, and probably the products of the reactions had not filled the existing voids.

When analyzing pores filled with internal reaction products of expansion and interface aggregate paste in Raman spectroscopy, spectra with wave numbers and peaks similar to those of crystalline products from ASR studied in [17, 19] were found.

Regardless of the origin of the microfissures in the concrete, the porosity of this material increase [14]. Water is a factor that contributes to the migration of sulfate ions [14], generating expansion reactions in different locations of a concrete structure.

The mechanisms of ASR and DEF reactions depend on the flow of liquids or gases in the microstructure, so for these internal expansion reactions to develop it is necessary to have connectivity between the pores [20]. For the progress of these reactions it was necessary to have preferential paths for the moisture to enter and then trigger the expansion in the concrete, filling free pores and later cracking the structure of the pile cap foundation. It is possible that there is still residual expansion in the concrete, and new tests are necessary to evaluate this characteristic.

4 Conclusions

Based on the cracks observed in-field and taking as reference the results of the studies and laboratory analysis in the concrete cores presented in this work, it can be stated that the concrete structure presents chemical changes that have affected its integrity. The most relevant conclusions of these studies are as follows:

- The physical–chemical characterization performed indicated that the pile cap foundation from which the specimens were extracted was affected by internal swelling reactions in the concrete, notably ASR and DEF;
- Among the two reactions referred to DEF proved to be more predominant and is, in the author's opinion, the main reason for the observed cracking;
- DEF possibly originated in the high hydration heat that may have occurred in the concreting of the important concrete volume of the pile cap block;
- The alkali-silica reaction was found in concrete through dispersive X-ray spectroscopy, with the presence of mineral components, such as silicon and quartz and by means of Raman spectroscopy, with a wave number of about 600 cm^{-1}, proving the presence of crystalline products of this reaction;
- The ettringite crystals that filled the pores were detected with the naked eye and by scanning electron microscopy and X-ray diffraction;
- The analysis with EDS obtained a predominance of sulfur, aluminum and calcium, being reaffirmed in the intensities of the XRD standards, where sulfate in the form of pyrite was found, as well as ettringite and calcite;
- Porosity values between 9 and 10% were also high, in accordance with their permeability and with the extensive pore network existing in the concrete.

References

1. Allahvedi A, Hashemi H (2015) Investigating the resistance of alkali-activated slag mortar exposed to magnesium sulfate attack. Int J Civ Eng 13(4A):379–387. https://doi.org/10.22068/IJCE.13.4.379
2. Machoviè V, Kopecký L, Němeček J, Kolář F, Svítilová J, Bittnar Z, Andertová J (2008) Raman micro-spectroscopy mapping and microstructural and micromechanical study of interfacial transition zone in concrete reinforced by poly (ethylene terephthalate) fibres. Ceramics Silikaty 52(1):54–60
3. Shayan A, Morris H (2004) Combined deterioration problems in a coastal bridge in NSW, Australia. In: Proceedings of the 12th international conference on alkali-aggregate reaction in concrete. International Academic Publishers, Beijing, China
4. Hasparyk NP (2005) Investigation of concretes affected by the alkali-aggregate reaction and advanced characterization of exudate gel. PhD Thesis, Federal University of Rio Grande do Sul, Brazil
5. Shayan A, Al-Mahaidi R, Xu A (2008) Durability and strength assessment of AAR-affected Bridge deck planks. In: Proceedings of the 13th international conference on alkali-aggregate reaction in concrete, Trondheim, Norway
6. Hasparyk NP, Kuperman SC, Torres JR (2012) Case study involving combined attack of AAR and DEF in building foundation concrete. In: Proceedings of the 54th Brazilian congress of concrete—CBC2012, Maceió, Brazil
7. Sanchez LFM, Drimalas T, Fournier B, Mitchell D, Bastien J (2018) Comprehensive damage assessment in concrete affected by different internal swelling reaction (ISR) mechanisms. Cem Concr Res 107:284–303
8. Torres IF (2016) Andrade (2016) risk analysis of the delayed ettringite formation in pile caps foundation in the metropolitan region of Recife—PE—Brasil. IBRACON J de Estruturas e Mater 9(3):357–394. https://doi.org/10.1590/S1983-41952016000300003

9. Metha PK, Monteiro PJM (2013) Concrete: microstructure, properties and materials 4 McGraw-Hill Education New York
10. Özcan A, Karakoç MB (2019) The Resistance of blast furnace slag- and ferrochrome slag-based geopolymer concrete against acid attack. Int J Civ Eng 17(10):1571–1583
11. Laboratoire Central des Ponts et Chaussées (2018) Guide technique—recommendations for preventing disorders due to delayed ettringite formation, Paris
12. Leemann A, Bernard L, Alahrache S, Winnefeld F (2015) ASR prevention—effect of aluminum and lithium ions on the reaction products. Cem Concr Res 76:192–201. https://doi.org/10.1016/j.cemconres.2015.06.002
13. Tahlaiti M (2010) Study of chloride penetration and corrosion initiation in saturated and tidal zones. PhD Thesis, La Rochelle University, France (in French)
14. Collepardi M (1999) Damage by delayed ettringite formation. Concr Int 21(1):69–74
15. Taylor HFW, Famy C, Scrivener KL (2001) Delayed ettringite formation. Cem Concr Res 31(5):683–693. https://doi.org/10.1016/S0008-8846(01)00466-5
16. Glasser FP, Damidot D, Atkins M (1995) Phase development in cement in relation to the secondary ettringite problem. Adv Cem Res 7(26):57–68. https://doi.org/10.1680/adcr.1995.7.26.57
17. Leemann A (2017) Raman microscopy of alkali-silica reaction (ASR) products formed in concrete. Cem Concr Res 102:41–47. https://doi.org/10.1016/j.cemconres.2017.08.014
18. Balachandran C, Muñoz JF, Arnold T (2017) Characterization of alkali silica reaction gels using Raman spectroscopy. Cem Concr Res 92:66–74. https://doi.org/10.1016/j.cemconres.2016.11.018
19. Merz C, Leemann A (2013) Assessment of the residual expansion potential of concrete from structures damaged by AAR. Cem Concr Res 52:182–189. https://doi.org/10.1016/j.cemconres.2013.07.001
20. Picandet V, Khelidj A, Bastian G (2001) Effect of axial compressive damage on gas permeability of ordinary and high-performance concrete. Cem Concr Res 31(11):1525–1532. https://doi.org/10.1016/S0008-8846(01)00546-4